PHILOSOPHICAL TRANSACTIONS A

rsta.royalsocietypublishing.org

Research

Cite this article: Sachdev S. 2016 Emergent gauge fields and the high-temperature superconductors. *Phil. Trans. R. Soc. A* **374**: 20150248.
http://dx.doi.org/10.1098/rsta.2015.0248

Accepted: 17 February 2016

One contribution of 7 to a discussion meeting issue 'Unifying physics and technology in light of Maxwell's equations'.

Subject Areas:
solid state physics, gauge theory

Keywords:
gauge fields, Luttinger theorem, quantum entanglement

Author for correspondence:
Subir Sachdev
e-mail: sachdev@g.harvard.edu

Speech presented at *Unifying physics and technology in light of Maxwell's equations*, Discussion Meeting at the Royal Society, London, 16–17 November 2015, celebrating the 150th anniversary of Maxwell's equations.

Emergent gauge fields and the high-temperature superconductors

Subir Sachdev[1,2]

[1]Department of Physics, Harvard University, Cambridge, MA 02138, USA
[2]Perimeter Institute for Theoretical Physics, Waterloo, Ontario, Canada N2L 2Y5

SS, 0000-0002-2432-7070

The quantum entanglement of many states of matter can be represented by electric and magnetic fields, much like those found in Maxwell's theory. These fields 'emerge' from the quantum structure of the many-electron state, rather than being fundamental degrees of freedom of the vacuum. I review basic aspects of the theory of emergent gauge fields in insulators in an intuitive manner. In metals, Fermi liquid (FL) theory relies on adiabatic continuity from the free electron state, and its central consequence is the existence of long-lived electron-like quasi-particles around a Fermi surface enclosing a volume determined by the total density of electrons, via the Luttinger theorem. However, long-range entanglement and emergent gauge fields can also be present in metals. I focus on the 'fractionalized Fermi liquid' (FL*) state, which also has long-lived electron-like quasi-particles around a Fermi surface; however, the Luttinger theorem on the Fermi volume is violated, and this requires the presence of emergent gauge fields, and the associated loss of adiabatic continuity with the free electron state. Finally, I present a brief survey of some recent experiments in the hole-doped cuprate superconductors, and interpret the properties of the pseudogap regime in the framework of the FL* theory.

This article is part of the themed issue 'Unifying physics and technology in light of Maxwell's equations'.

THE ROYAL SOCIETY PUBLISHING

1. Introduction

The copper-based high-temperature superconductors have provided a fascinating and fruitful environment for the study of quantum correlations in many-electron systems for over two decades. Significant experimental and theoretical advances have appeared at a steady pace over the years. In this article, I will review some theoretical background, and use it to interpret some remarkable recent experiments [1–8]. In particular, I argue that modern theoretical ideas on long-range quantum entanglement and emergent gauge fields provide a valuable framework for understanding the experimental results. I will discuss experimental signatures of quantum phases with emergent gauge fields, and their connections to the recent observations.

The common feature of all the copper-based superconductors is the presence of a square lattice of Cu and O atoms shown in figure 1*a*. For the purposes of this article, we can regard the O p orbitals as filled with pairs of electrons and inert. Only one of the Cu orbitals is active, and in a parent insulating compound, this orbital has a density of exactly one electron per site. The rest of this article will consider the physical properties of this Cu orbital residing on the vertices of a square lattice. It is customary to measure the density of electrons relative to the parent insulator with one electron per site: we will use p to denote the hole density: i.e. such a state has a density of $1-p$ electrons per Cu site. A recent schematic phase diagram of the hole-doped superconductor YBCO is shown in figure 1*b* as a function of p and the temperature T. The initial interest in these compounds was sparked by the presence of high-temperature superconductivity, indicated by the large values of T_c in figure 1*b*. However, I will not discuss the origin of this superconductivity in this article. Rather, the focus will be on the other phases, and in particular, the pseudogap metal (PG in figure 1*b*): the physical properties of this metal differ qualitatively from those of conventional metals, and so are of significant intrinsic theoretical interest. Furthermore, superconductivity appears as a low-temperature instability of the pseudogap, so a theory of the high value of T_c can only appear after a theory of the PG metal.

We begin our discussion by describing the simpler phases at the extremes of p in figure 1*b*.

At (and near) $p=0$, we have the antiferromagnet (AF) which is sketched in figure 2*a*. The Coulomb repulsion between the electrons keeps their charges immobile on the Cu lattice sites, so that each site has exactly one electron. The Coulomb interaction is insensitive to the spin of the electron, and so it would appear that each electron spin is free to rotate independently on each site. However, there are virtual 'superexchange' processes which induce terms in the effective Hamiltonian which prefer opposite orientations of nearest-neighbour spins, and the optimal state turns out to be the AF sketched in figure 2*a*. In this state, the spins are arranged in a chequerboard pattern, so that all the spins in one sublattice are parallel to each other, and antiparallel to spins on the other sublattice. Two key features of this AF state deserve attention here. (i) The state breaks a global spin rotation symmetry, and essentially all of its low-energy properties can be described by well-known quantum field theory methods associated with spontaneously broken symmetries. (ii) The wavefunction does not have long-range entanglement, and the exact many-electron wavefunction can be obtained by a series of local unitary transformations on the simple product state sketched in figure 2*a*.

At the other end of larger values of p, we have the Fermi liquid (FL) phase. This is a metallic state, in which the electronic properties are most similar to those of simple monoatomic metals like sodium or gold. This is also a quantum state without long-range entanglement, and the many-electron wavefunction can be well approximated by a product over single-electron momentum eigenstates (Bloch waves); note the contrast from the AF state, where the relevant single-particle states were localized on single sites in position space. We will discuss some further important properties of the FL state in §3.

Section 2 will describe possible insulating states on the square lattice, other than the simple AF state found in the cuprate compounds at $p=0$. The objective here will be to introduce states with long-range quantum entanglement in a simple setting, and highlight their connection to emergent gauge fields. Then §4 will combine the descriptions of §§3 and 2 to propose a metallic state with long-range quantum entanglement and emergent gauge fields: the fractionalized Fermi liquid

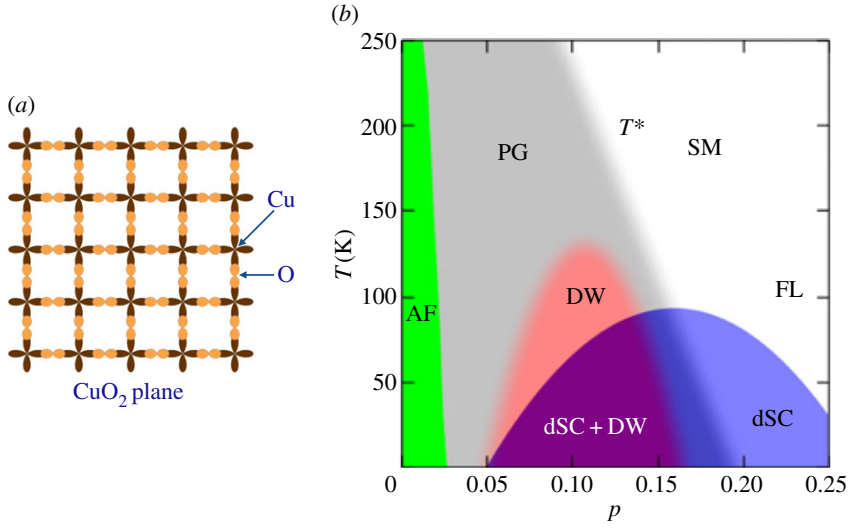

Figure 1. (*a*) The square lattice of Cu and O atoms found in every copper-based high-temperature superconductor. (*b*) A schematic phase diagram of the YBCO superconductors as a function of the hole density p and the temperature T; adapted from [6]. The phases are discussed in the text: AF, insulating antiferromagnet; PG, pseudogap; DW, density wave; dSC, *d*-wave superconductor; SM, strange metal; FL, Fermi liquid. The critical temperature for superconductivity is T_c, and T^* is the boundary of the pseudogap regime.

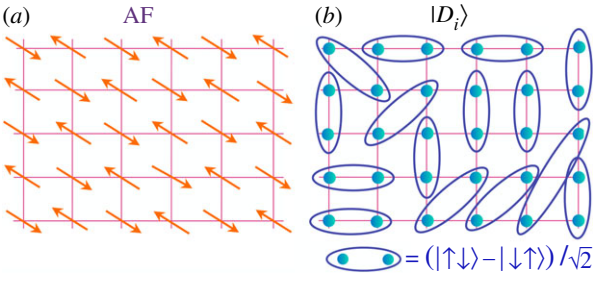

Figure 2. (*a*) The insulating AF state at $p = 0$. (*b*) Component of a 'resonating valence bond' wavefunction for the AF which preserves spin rotation symmetry; all the $|D_i\rangle$ in equation (2.1) have similar pairings of electrons on nearby sites (not necessarily nearest neighbours). (Online version in colour.)

(FL*). Finally, in §5, we will review the evidence from recent experiments that the pseudogap (PG) regime of figure 1*b* is described by an FL* phase.

I also note here another recent review article [9], which discusses similar issues at a more specialized level aimed at condensed matter physicists. The gauge theories of the insulators discussed in §2 were reviewed in earlier lectures [10,11].

2. Emergent gauge fields in insulators

The spontaneously broken spin rotation symmetry of the AF state at $p = 0$ is not observed at higher p. This section will, therefore, describe quantum states which preserve spin rotation symmetry. However, in the interests of theoretical simplicity, we will discuss such states in the insulator at the density of $p = 0$, and assume that the AF state can be destabilized by suitable further-neighbour superexchange interactions between the electron spins.

We begin with the 'resonating valence bond' (RVB) state

$$|\Psi\rangle = \sum_i c_i |D_i\rangle, \tag{2.1}$$

where i extends over all possible pairings of electrons on nearby sites, and a state $|D_i\rangle$ associated with one such pairing is shown in figure 2*b*; the c_i are complex coefficients that we will leave unspecified here. Note that the electrons in a valence bond need not be nearest neighbours. Each $|D_i\rangle$ is a spin singlet, and so spin rotation invariance is preserved; the AF exchange interaction is optimized between the electrons within a single valence bond, but not between electrons in separate valence bonds. We also assume that the c_i respect the translational and other symmetries of the square lattice. Such a state was first proposed by Pauling [12] as a description of a simple metal like lithium. We now know that Pauling's proposal is incorrect for such metals. But we will return to a variant of the RVB state in §4 which does indeed describe a metal, and this metal will be connected to the phase diagram of the cuprates in §5. Anderson revived the RVB state many years later [13] as a description of Mott insulators: these are materials with a density of one electron per site, which are driven to be insulators by the Coulomb repulsion between the electrons (contrary to the Bloch theorem for free electrons, which requires metallic behaviour at this density).

In a modern theoretical framework, we now realize that the true significance of the Pauling–Anderson RVB proposal was that it was the first quantum state to realize *long-range* quantum entanglement. Similar entanglement appeared subsequently in Laughlin's wavefunction for the fractional quantum Hall state [14], and for RVB states in the absence of time-reversal symmetry [15]. The long-range nature of the entanglement can be made precise by computation of the 'topological entanglement entropy' [16–18]. But here we will be satisfied by a qualitative description of the sensitivity of the spectrum of states to the topology of the manifold on which the square lattice resides. The sensitivity is present irrespective of the size of the manifold (provided it is much larger than the lattice spacing), and so indicates that the information on the quantum entanglement between the electrons is truly long-ranged. A wavefunction which is a product of localized single-particle states would not care about the global topology of the manifold.

The basic argument on the long-range quantum information contained in the RVB state is summarized in figure 3. Place the square lattice on a very large torus (i.e. impose periodic boundary conditions in both directions), draw an arbitrary imaginary cut across the lattice, indicated by the red line, and count the number of valence bonds crossing the cut. It is not difficult to see that any *local* rearrangement of the valence bonds will preserve the number of valence bonds crossing the cut modulo 2. Only very non-local processes can change the parity of the valence bonds crossing the cut: one such process involves breaking a valence bond across the cut into its constituent electrons, and moving the electrons separately around a cycle of the torus crossing the cut, so that they meet on the other side and form a new valence bond which no longer crosses the cut (figure 4). Ignoring this very non-local process, we see that the Hilbert space splits into disjoint sectors, containing states with even or odd number of valence bonds across the cut [19,20]. Locally, the two sectors are identical, and so we expect the two sectors to have ground states (and also excited states) of nearly the same energy for a large enough torus. The presence of these near-degenerate states is dependent on the global spatial topology, i.e. it requires periodic boundary conditions around the cycles of the torus, and so can be viewed as a signature of long-range quantum entanglement.

The above description of topological degeneracy and entanglement relies on a somewhat arbitrary and imprecise trial wavefunction. A precise understanding is provided by a formulation of the physics of RVB in terms of an emergent gauge theory. Such a formulation provides another way to view the nearly degenerate states obtained above on a torus: they are linear combinations of states obtained by inserting fluxes of the emergent gauge fields through the cycles of the torus.

The formulation as a gauge theory [21,22] becomes evident upon considering a simplified model with valence bonds only between nearest-neighbour sites on the square lattice. We introduce valence bond number operators $\hat{n}$ on every nearest-neighbour link, and then there is a crucial constraint that there is exactly one valence bond emerging from every site, as illustrated

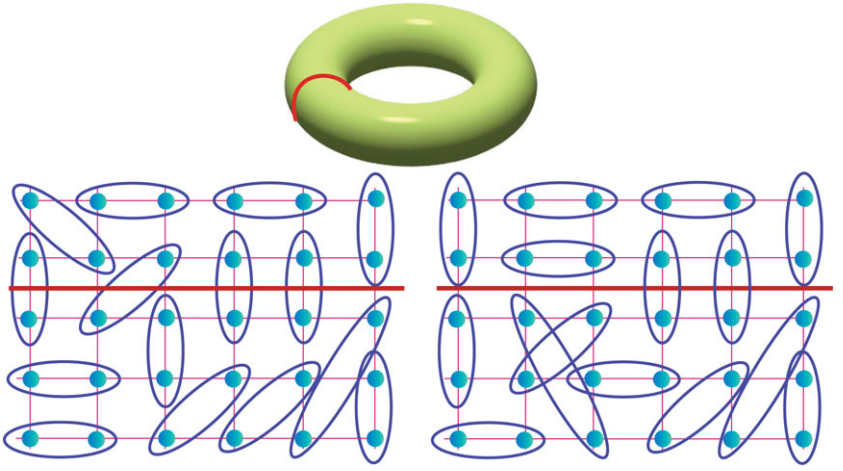

Figure 3. Sensitivity of the RVB state to the torus geometry: the number of valence bonds crossing the cut (red line) can only differ by an even integer between any two configurations (like those shown) which differ by an arbitrary local arrangement of valence bonds. (Online version in colour.)

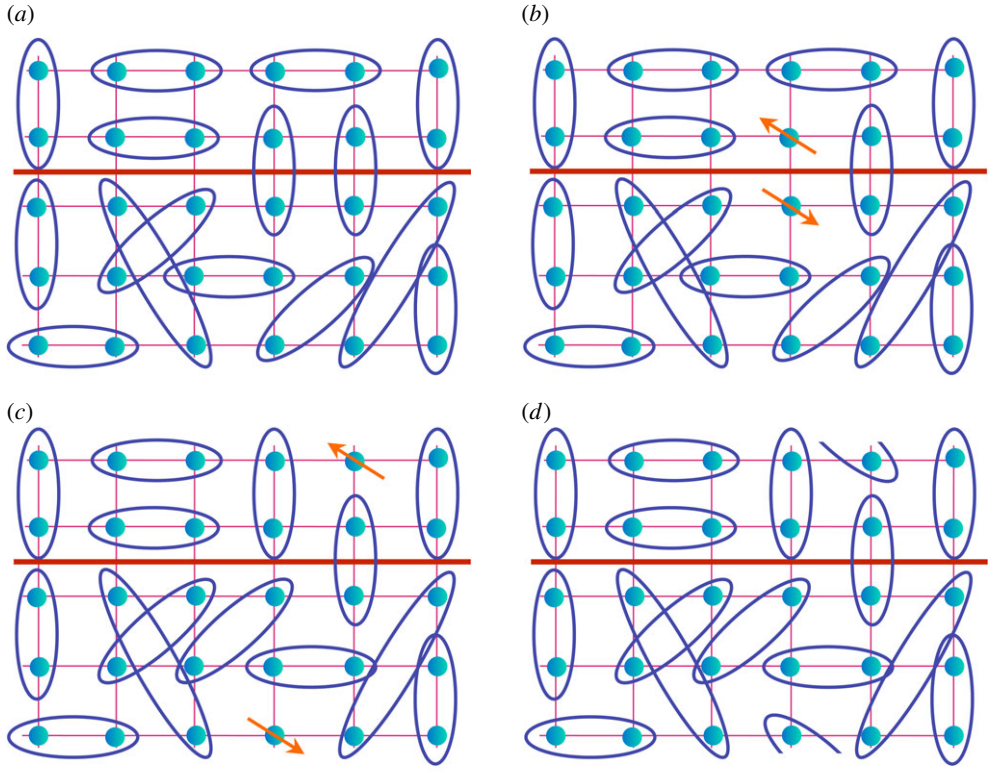

Figure 4. (*a–d*) Non-local process which changes the parity of the number of valence bonds crossing the cut. A valence bond splits into two spins, which pair up again after going around the torus. (Online version in colour.)

in figure 5*a*. After introducing oriented 'electric field' operators $\hat{E}_{i\alpha} = (-1)^{i_x+i_y}\hat{n}_{i\alpha}$ (here i labels sites of the square lattice and $\alpha = x, y$ labels the two directions), this local constraint can be written in the very suggestive form

$$\Delta_\alpha \hat{E}_{i\alpha} = \rho_i, \tag{2.2}$$

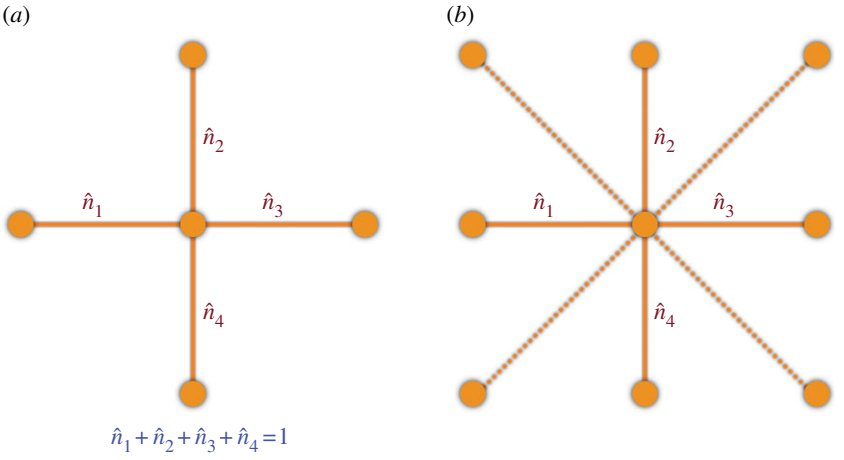

Figure 5. (*a*) Nearest-neighbour valence bond number operators, proportional to the electric field of a compact U(1) gauge theory. (*b*) Model with valence bonds connecting the same sublattice: now the constraint on the number operators is modified, and the spin liquid is described by a $\mathbb{Z}_2$ gauge theory. (Online version in colour.)

where Δ_α is a discrete lattice derivative, and $\rho_i \equiv (-1)^{i_x+i_y}$ is a background 'charge' density. Equation (2.2) is analogous to Gauss's law in electrodynamics, and a key indication that the physics of resonating valence bonds is described by an emergent gauge theory. An important difference from Maxwell's U(1) electrodynamics is that the eigenvalues of the electric field operator $\hat{E}_{i\alpha}$ must be integers. In terms of the canonically conjugate gauge field $\hat{A}_{i\alpha}$,

$$[\hat{A}_{i\alpha}, \hat{E}_{j\beta}] = \mathrm{i}\hbar\delta_{ij}\delta_{\alpha\beta}, \tag{2.3}$$

the integral constraint translates into the requirement that $\hat{A}_{i\alpha}$ is a compact angular variable on a unit circle and that $\hat{A}_{i\alpha}$ and $\hat{A}_{i\alpha} + 2\pi$ are equivalent. So there is an equivalence between the quantum theory of nearest-neighbour resonating valence bonds on a square lattice, and compact U(1) electrodynamics in the presence of fixed background charges ρ_i. A non-perturbative analysis of such a theory shows [23,24] that ultimately there is no gapless 'photon' associated with the emergent gauge field $\hat{A}$: compact U(1) electrodynamics is confining in two spatial dimensions, and in the presence of the background charges the confinement leads to valence bond solid (VBS) order illustrated in figure 6. The VBS state breaks square lattice rotation symmetry, and all excitations of the AF, including the incipient photon, have an energy gap. In subsequent work, it was realized that the gapless photon can re-emerge at special 'deconfined' critical points [25–27] or phases [28], even in two spatial dimensions. In particular, in certain models with a quantum phase transition between a VBS state and the ordered AF in figure 2*a* [23–25], the quantum critical point supports a gapless photon (along with gapless matter fields). This is illustrated in figure 6*b* by numerical results of Sandvik [29]: the circular distribution of valence bonds is evidence for an emergent continuous lattice rotation symmetry, and the associated Goldstone mode is the dual of the photon.

Although U(1) gauge theory does realize spin liquids with long-range entanglement and emergent photons, the gaplessness and 'criticality' of the spin liquids indicates the presence of long-range valence bonds, and the Pauling–Anderson trial wavefunctions are poor descriptions of such states. However, it was argued [30–34] that a stable deconfined gauge theory with an energy gap and short-range valence bonds can be obtained in models with valence bonds which connect sites on the same sublattice, as shown in figure 5*b*, because the same-sublattice bonds act like charge ± 2 Higgs fields in the compact U(1) gauge theory. In such gauge theories [35,36], there can be a 'Higgs' phase, which realizes a stable, gapped, RVB state preserving all symmetries of the Hamiltonian, including time reversal, described by an emergent $\mathbb{Z}_2$ gauge theory [31,34]. The $\mathbb{Z}_2$

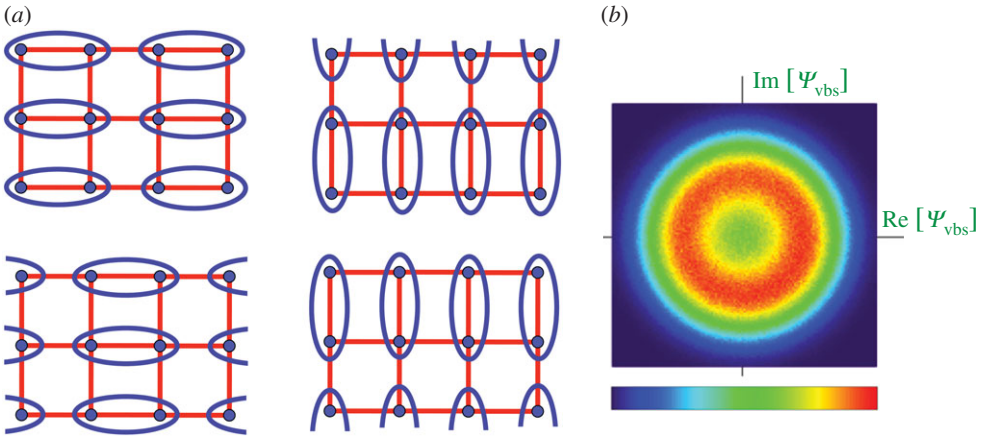

Figure 6. (*a*) The four VBS states which break square lattice rotational symmetry. (*b*) Distribution of the complex VBS order parameter $\Psi_{\rm vbs}$ in the quantum Monte Carlo study by Sandvik [29]; the real and imaginary parts of this order measure the probability of the VBS states in the first and second columns. The near-circular distribution of $\Psi_{\rm vbs}$ reflects an emergent symmetry which is a signature of the existence of a photon.

gauge theory can be viewed as a discrete analogue of the compact U(1) theory in which the gauge field takes only two possible values $\hat{A}_{i\alpha} = 0, \pi$. The intimate connection between a spin liquid with a deconfined $\mathbb{Z}_2$ gauge field, and a non-bipartite RVB trial wavefunction like equation (2.1), was shown convincingly by Wildeboer *et al.* [18]. Upon varying parameters in the underlying Hamiltonian, the $\mathbb{Z}_2$ spin liquid can undergo a confinement transition to a VBS phase which is described by a dual frustrated Ising model [31,34].

3. The Fermi liquid

We now turn to the metallic state found at large p (above the superconducting T_c) in figure 1*b*. This is the familiar FL, similar to that found in simple metals like sodium or gold.

The key properties of an FL, reviewed in many textbooks, are:

— The FL state of interacting electrons is adiabatically connected to the free electron state. The ground state of free electrons has a Fermi surface in momentum space, which separates the occupied and empty momentum eigenstates. This Fermi surface is also present in the interacting electron state, and the low-energy excitations are long-lived, electron-like quasi-particles near the Fermi surface.

— The Luttinger theorem states that the volume enclosed by the Fermi surface (i.e. the Fermi volume) is equal (modulo phase space factors we ignore here) to the total density of electrons. This equality is obviously true for free electrons, but is also proved to be true, to all orders in the interactions, for any state adiabatically connected to the free electron state.

— For simple convex Fermi surfaces, the Fermi volume can be measured by the Hall coefficient, $R_{\rm H}$, measuring the transverse voltage across a current in the presence of an applied magnetic field. We have $1/(eR_{\rm H}) = -$(electron density) for electron-like Fermi surfaces, and $1/(eR_{\rm H}) =$ (hole density) for hole-like Fermi surfaces.

For the cuprates, the FL is obtained by removing a density, p, of electrons from the insulating AF, as shown in figure 7*a*. Relative to the fully filled state with two electrons on each site (figure 7*b*), this state has a density of holes equal to $1 + p$. Hence the FL state without AF order can have a single hole-like Fermi surface with a Fermi volume of $1 + p$ (and *not* p). And indeed, just such a

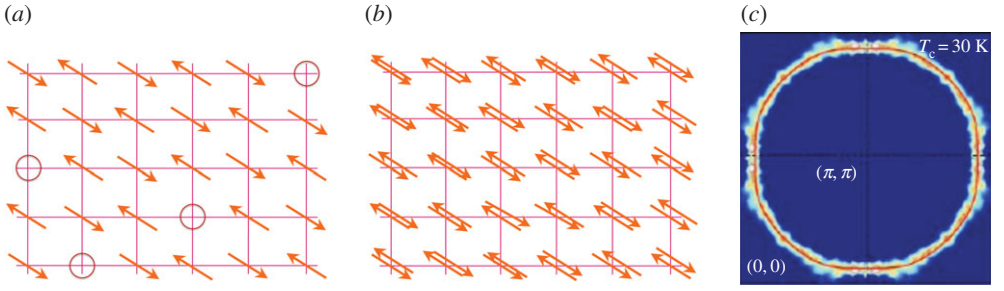

Figure 7. (*a*) State obtained after removing electrons with density p from the AF state in figure 2*a*. Relative to the fully filled state with two electrons per site in (*b*), this state has a density of holes equal to $1 + p$. (*c*) Photoemission results from Platé *et al.* [37] showing a Fermi surface of size $1 + p$ in the FL region of figure 1*b*. This is the expected Luttinger volume at this density, in a state without any AF order.

Fermi surface is observed in photoemission experiments in the cuprates (figure 7*c*) in the region marked FL in figure 1*b*.

4. Emergent gauge fields in a metal: the fractionalized Fermi liquid

Next, we turn our attention to the smaller p region marked PG (pseudogap) in figure 1*b*. We will review the experimental observations in this region in §5, but for now we note that in many respects this region behaves like an ordinary FL, but with the crucial difference that the density of charge carriers is p and not the Luttinger density of $1 + p$. So here we ask the theoretical question: is it possible to obtain an FL which violates the Luttinger theorem and has a Fermi surface of size p of electron-like quasi-particles? From the structure of the Luttinger theorem we know that any such state cannot be adiabatically connected to the free electron state. A key result is that long-range quantum entanglement and associated emergent gauge fields are *necessary* characteristics of metallic states which violate the Luttinger theorem, and these also break the adiabatic connection to the free electron state [38,39].

(There are claims [40] that zeros of electron Green's functions can be used to modify the Luttinger result. I believe such results are artefacts of simplified models. Such zeros do not generically exist as lines in the Brillouin zone (in two dimensions) for gapless states because both the real and imaginary parts of the Green's functions have to vanish.)

One way to obtain a metal with carrier density p and without AF order is to imagine that the electron spins in figure 7*a* pair up into resonating valence bonds, rather like the insulator in figure 2*b*. This is illustrated in figure 8*a*; the resonance between the valence bonds can now allow processes in which the vacant sites can move, as shown in figure 8*b*. As this process now transfers physical charge, the resulting state can be expected to be an electrical conductor. A subtle computation is required to determine the quantum statistics obeyed by the mobile vacancies, but, depending upon the parameter regimes, it can be either bosonic or fermionic [41,42]. Assuming fermionic statistics, we have the possibility that the vacancies will form a Fermi surface, realizing a metallic state. Note that the vacancies do not transport spin, and such spinless charge carriers are often referred to as 'holons'; the metallic state we have postulated is a holon metal. The low-energy quasi-particles near the Fermi surface of the holon metal will also be holons, carrying unit electrical charge but no spin. Consequently, such quasi-particles are not directly observable in photoemission experiments, which necessarily eject bare electrons with both charge and spin. As low-energy electronic quasi-particles are observed in photoemission studies of the PG region in the cuprates (see §5), the holon metal is not favoured as a candidate for the PG metal.

To obtain a spinful quasi-particle, we clearly have to attach an electronic spin to each holon. And as shown in figure 9, it is not difficult to imagine conditions under which this might be

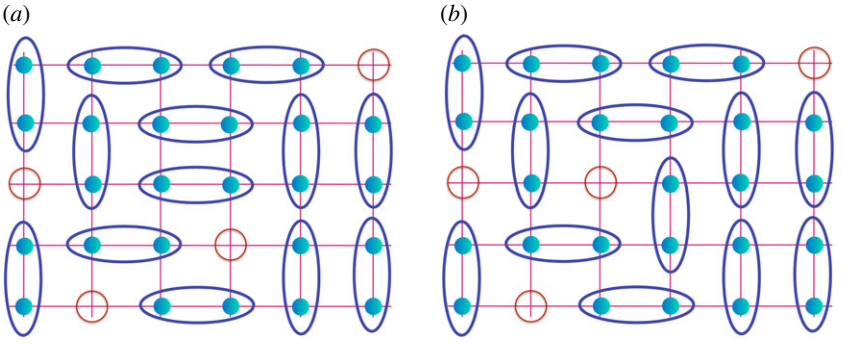

Figure 8. (*a*) State obtained by pairing the spins in figure 7*a* into valence bonds. (*b*) Resonance between the valence bonds leads to the motion of the vacancy in the centre of the figure. The mobile vacancy is a 'holon', carrying unit charge but no spin. If the holons have fermionic statistics, such a mobile holon state can realize a holon metal. Only nearest-neighbour pairs of spins are shown for simplicity. (Online version in colour.)

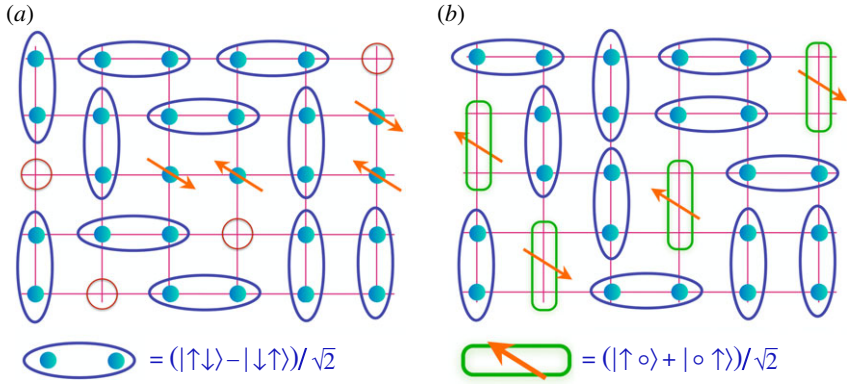

Figure 9. (*a*) State obtained by breaking density $p/2$ valence bonds in figure 8*a* into their constitutent spinons. (*b*) The spinons move into the neighbourhood of the vacancies and form holon–spinon bound states represented by the green rectangular dimers [43]. The state with resonating blue elliptical and green rectangular dimers realizes a metal with a Fermi volume of p quasi-particles with charge $+e$ and spin $S = \frac{1}{2}$: the fractionalized Fermi liquid (FL*). (Online version in colour.)

favourable: (i) We break density $p/2$ valence bonds into their constituent spins (figure 9*a*); this costs some exchange energy for each valence bond broken. (ii) We move the constituent spins (spinons) into the neighbourhood of the holons. (iii) The holons and spinons form a bound state (figure 9*b*) which has both charge $+e$ and spin $S = \frac{1}{2}$, the same quantum numbers as (the absence of) an electron; this bound state formation gains energy which can offset the energy cost of (i). We now have a modified resonating valence bond state [43], like that in equation (2.1), but with $|D_i\rangle$ consisting of pairing of sites of the square lattice with two categories of 'valence bonds': the blue and green dimers in figure 9*b*. The first class (blue) is the same as the electron singlet pairs found in the Pauling–Anderson state. The second class (green) consists of a single electron resonating between the two sites at the ends of the bond. From their constituents, it is clear that, relative to the insulating RVB state, the blue dimers are spinless, charge-neutral bosons, while the green dimers are spin $S = \frac{1}{2}$, charge $+e$ fermions. Evidence that the states associated with the blue and green dimers dominate the wavefunction of the lightly doped cuprates appears in cluster dynamical mean-field studies [44,45]. Both classes of dimers are mobile, and the situation is somewhat analogous to a ^{4}He–^{3}He mixture. Like the ^{3}He atoms, the green fermions can form

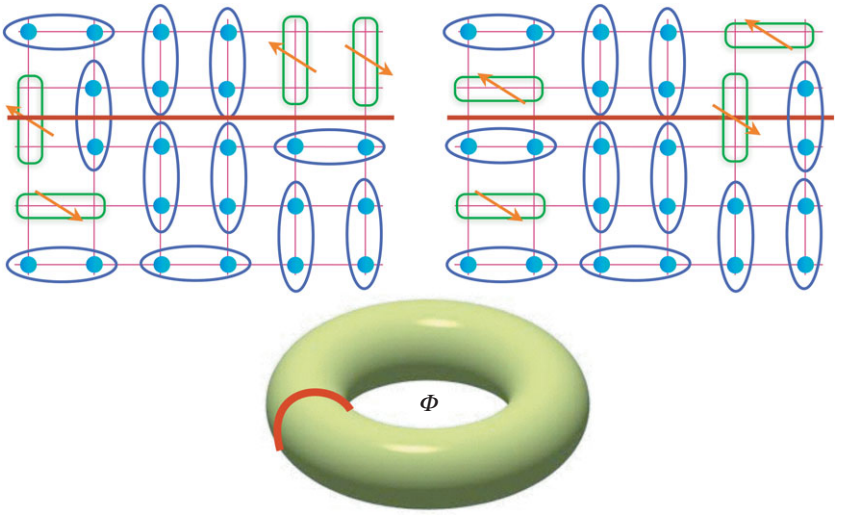

Figure 10. Sample configurations of the wavefunction of the FL* state. The two configurations differ by local rearrangements which preserve the sum of the number of blue elliptical *and* green rectangular dimers crossing the cut modulo 2, just as in figure 3 (only nearest-neighbour dimers are shown for simplicity). This conservation implies the presence of gauge excitations, and additional states sensitive to the global topology, which cannot be decomposed into the quasi-particle excitations around the Fermi surface. Arguments in [38,39,57], based upon the adiabatic insertion of a fluxoid $\Phi = h/e$ through a cycle of the torus, show that the presence of these states allows the Fermi volume to take a non-Luttinger value. (Online version in colour.)

a Fermi surface, and extension of the Luttinger argument to the present situation shows that the Fermi volume is exactly p [38,46,47]. However, unlike the ^{4}He–^{3}He mixture, superfluidity is not immediate, because of the close-packing constraint on the blue + green dimers; onset of superfluidity will require pairing of the green dimers and will not be explored here. So the state obtained by resonating motion of the dimers in figure 9*b* is a metal, dubbed the FL* [46]. It has a Fermi volume of p, with well-defined electron-like quasi-particles near the Fermi surface.

A metallic state with a Fermi volume of density p holes with charge $+e$ and spin $S = \frac{1}{2}$ was initially described in [48,49] by considering a theory for the loss of AF order in a doped AF state like that in figure 7*a*. Numerous later studies [43,47,50–56] described the resulting metallic state more completely in terms of the binding of holons and spinons, similar to the discussion above. These studies also showed the presence of the emergent gauge excitations in the metal.

We can also see the presence of emergent gauge fields, and associated low-energy states sensitive to the topology of the manifold, in our simplified description here of the FL* metal. Indeed, such low-energy states are required to evade the Luttinger theorem on the Fermi surface volume [38,39]. The FL* metal shares its topological features with corresponding insulating spin liquids, and we can transfer all of the arguments of §2 practically unchanged, merely by applying them to wavefunctions like figure 9*b* in a 'colour blind' manner. So the arguments in figure 3 on the conservation of the number of valence bonds across the cut modulo 2, and associated near-degeneracies on the torus, apply equally to the FL* wavefunction after counting the numbers of *both* blue and green dimers (figure 10). The presence of these near-degenerate topological states is also crucial for the Luttinger-volume-violating Fermi surface. Oshikawa [57] presented a proof of the Luttinger volume in an FL by considering the consequences of adiabatically inserting a fluxoid $\Phi = h/e$ through a cycle of the torus, while assuming that the only low-energy excitations on the torus are the quasi-particles around the Fermi surface. However, with the availability of the low-energy topological states discussed in figure 10, which are not related to quasi-particle excitations, it is possible to modify Oshikawa's proof and obtain a Fermi volume different from the Luttinger volume [38,39]; indeed, a Luttinger volume of p holes appears naturally in many models, including the simple models discussed here.

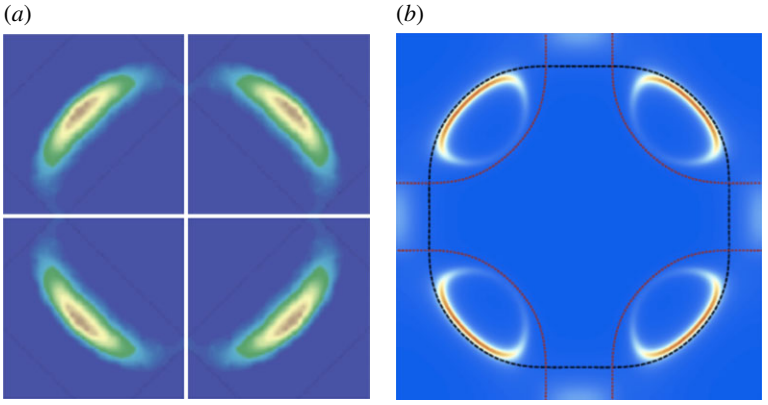

Figure 11. (*a*) Photoemission spectrum in the PG regime [58]. Shown is the first Brillouin zone of the square lattice centred at (π, π), as in figure 7*c*. However, unlike the FL result in figure 7*c*, there is no continuous Fermi surface, only 'Fermi arcs'. (*b*) Photoemission from an FL* model in [54]. The Fermi surface consists of hole pockets of total area p, with intensity enhanced along the observed Fermi arcs, but suppressed on the 'back' sides of the pockets.

To summarize, this section has presented a simple description of a metallic state with the following features:

— a Fermi surface of holes of charge e and spin $S = \frac{1}{2}$ enclosing volume p, and not the Luttinger volume of $1 + p$;
— additional low-energy quantum states on a torus not associated with quasi-particle excitations, i.e. emergent gauge fields.

The flux-piercing arguments in [38,39] show that it is not possible to have the first feature without the second.

5. The pseudogap metal of the cuprates

An early indication of the mysterious nature of the PG regime in figure 1*b* was its remarkable photoemission spectrum [58,59] (figure 11). There are low-energy electronic excitations along the 'nodal' directions in the form of 'Fermi arcs', but none in the antinodal directions. In the FL* proposal, these arcs are remnants of hole pockets centred on the Brillouin zone diagonals, with intensity suppressed on the 'back' sides of the pockets [40,54], as shown in figure 11. The complete hole pockets have not been observed in photoemission, but this is possibly accounted for by thermal broadening and weak intensity on their 'back' sides.

More persuasive evidence for the FL* interpretation of the PG phase has come from a number of other experiments:

— A T-independent positive Hall coefficient R_H corresponding to carrier density p in the higher-temperature pseudogap [60]. This is the expected Hall coefficient of the hole pockets in the FL* phase.
— The frequency and temperature dependence of the optical conductivity has an FL form $\sim 1/(-i\omega + 1/\tau)$ with $1/\tau \sim \omega^2 + T^2$ [1]. This FL form is present although the overall prefactor corresponds to a carrier density p.
— Magnetoresistance measurements obey Kohler's rule [2] with $\rho_{xx} \sim \tau^{-1}(1 + aH^2T^2)$, again as expected by the Fermi pocket of long-lived quasi-particles.
— Density wave (DW) modulations have long been observed in STM experiments [61] in the region marked DW in figure 1*b*. Following theoretical proposals [62,63], a number of experiments [3–7] have identified the pattern of modulations as a d-form factor DW.

Computations of DW instabilities of the FL* metal lead naturally to a *d*-form factor DW, with a wavevector similar to that observed in experiments [64].

— Finally, very interesting recent measurements by Badoux *et al.* [8] of the Hall coefficient at high fields and low T for $p \approx 0.16$ in YBCO clearly show the absence of DW order, unlike those at lower p. Furthermore, unlike the DW region, the Hall coefficient remains positive and corresponds to a density of p carriers. Only at higher $p \approx 0.19$ does the FL Hall coefficient of $1 + p$ appear. A possible explanation is that the FL* phase is present in the doping regime $0.16 < p < 0.19$ without the appearance of DW order. In figure 1*b*, this corresponds to the T^* boundary extending past the DW region at low T.

6. Conclusion

We have described here the striking difference between the metallic states at low and high hole density, p, in the cuprate superconductors (figure 1*b*). A theory for these states, and for the crossover between them, is clearly a needed precursor to any quantitative understanding of the high value of T_c for the onset of superconductivity.

At high p, there is strong evidence for a conventional FL state. This is an 'unentangled' state, and its wavefunction is adiabatically connected to the free electron state which is a product of single-particle Bloch waves. The Fermi surface has long-lived fermionic excitations with charge $+e$ and spin $S = \frac{1}{2}$. The volume enclosed by the Fermi surface is $1 + p$, and this obeys Luttinger's theorem. Such a Fermi surface is seen clearly in photoemission experiments [37], and also by the value of the Hall coefficient [8].

At low p, in the PG regime, the experimental results pose many interesting puzzles. Numerous transport measurements [1,2,60], and also the remarkable recent Hall coefficient measurements of Badoux *et al.* [8] at low T and $p \approx 0.16$, are consistent with the presence of an FL, but with a Fermi volume of p, which is not the Luttinger value. We described basic aspects of the theory of the FL* which realizes just such a Fermi surface. Long-range quantum entanglement and emergent gauge fields are necessary ingredients which allow the FL* metal to have a Fermi surface enclosing a non-Luttinger volume. The FL* metal also leads to a possible understanding [64] of the DW order found at low temperatures in the pseudogap regime [3–7].

Assuming the presence of distinct FL and FL* metals at high and low p, we are faced with the central open problem of connecting them at intermediate p. Although neither metal has a broken symmetry, the presence of emergent gauge fields in the FL* implies that there cannot be an adiabatic connection between the FL* and FL phases at zero temperature. So a quantum phase transition must be present, but it is not in the Landau–Ginzburg–Wilson symmetry-breaking class. We need a quantum critical theory with emergent gauge fields for the FL–FL* transition, and this can possibly provide an explanation for the intermediate strange metal (SM) noted in figure 1*b*. Examples of FL–FL* critical theories have been proposed [38,65], but a deeper understanding of such theories and their connections to experimental observations in the SM remain important challenges for future research.

Competing interests. The author declares that he has no competing interests.

Funding. This research was supported by the NSF under grant DMR-1360789. Research at Perimeter Institute is supported by the Government of Canada through Industry Canada and by the Province of Ontario through the Ministry of Research and Innovation.

Acknowledgements. I thank Andrea Allais, Debanjan Chowdhury, Séamus Davis, Kazu Fujita, Antoine Georges, Mohammad Hamidian, Cyril Proust, Matthias Punk and Louis Taillefer for numerous fruitful discussions on theories, experiments and their connections.

References

1. Mirzaei SI *et al.* 2013 Spectroscopic evidence for Fermi liquid-like energy and temperature dependence of the relaxation rate in the pseudogap phase of the cuprates. *Proc. Natl Acad. Sci. USA* **110**, 5774–5778. (doi:10.1073/pnas.1218846110)

2. Chan MK *et al.* 2014 In-plane magnetoresistance obeys Kohler's rule in the pseudogap phase of cuprate superconductors. *Phys. Rev. Lett.* **113**, 177005. (doi:10.1103/PhysRevLett.113.177005)
3. Fujita K *et al.* 2014 Direct phase-sensitive identification of a *d*-form factor density wave in underdoped cuprates. *Proc. Natl Acad. Sci. USA* **111**, 3026–3031. (doi:10.1073/pnas.1406297111)
4. Comin R *et al.* 2015 Symmetry of charge order in cuprates. *Nat. Mater.* **14**, 796–800. (doi:10.1038/nmat4295)
5. Forgan EM *et al.* 2015 The microscopic structure of charge density waves in underdoped $YBa_2Cu_3O_{6.54}$ revealed by X-ray diffraction. *Nat. Commun.* **6**, 10064. (doi:10.1038/ncomms10064)
6. Hamidian MH *et al.* 2015 Atomic-scale electronic structure of the cuprate *d*-symmetry form factor density wave state. *Nat. Phys.* **12**, 150156. (doi:10.1038/nphys3519)
7. Hamidian MH *et al.* 2015 Magnetic-field induced interconversion of Cooper pairs and density wave states within cuprate composite order. (http://arxiv.org/abs/1508. 00620 [cond-mat.supr-con])
8. Badoux S *et al.* 2016 Change of carrier density at the pseudogap critical point of a cuprate superconductor. *Nature* **531**, 210–214. (doi:10.1038/nature16983)
9. Chowdhury D, Sachdev S. 2015 The enigma of the pseudogap phase of the cuprate superconductors. In *Quantum criticality in condensed matter: Phenomena, materials and ideas in theory and experiment*. 50th Karpacz Winter School of Theoretical Physics, Karpacz, Poland, 2–9 March 2014 (ed. J Jędrzejewski), pp. 1–43. Singapore: World Scientific. (doi:10.1142/9789814704090_0001)
10. Sachdev S. 2004 Quantum phases and phase transitions of Mott insulators. In *Quantum magnetism* (eds U Schollwöck, J Richter, DJJ Farnell, RF Bishop). Lecture Notes in Physics, vol. 645, pp. 381–432. Berlin, Germany: Springer.
11. Sachdev S. 2012 Quantum phase transitions of antiferromagnets and the cuprate superconductors. In *Modern theories of many-particle systems in condensed matter physics* (eds DC Cabra, A Honecker, P Pujol). 2009 Les Houches School, Lecture Notes in Physics, vol. 843, pp. 1–51. Berlin, Germany: Springer.
12. Pauling L. 1949 A resonating-valence-bond theory of metals and intermetallic compounds. *Proc. R. Soc. Lond. A* **196**, 343–362. (doi:10.1098/rspa.1949.0032)
13. Anderson PW. 1973 Resonating valence bonds: a new kind of insulator? *Mater. Res. Bull.* **8**, 153–160. (doi:10.1016/0025-5408(73)90167-0)
14. Laughlin RB. 1983 Anomalous quantum Hall effect: an incompressible quantum fluid with fractionally charged excitations. *Phys. Rev. Lett.* **50**, 1395–1398. (doi:10.1103/PhysRevLett.50.1395)
15. Kalmeyer V, Laughlin RB. 1987 Equivalence of the resonating-valence-bond and fractional quantum Hall states. *Phys. Rev. Lett.* **59**, 2095–2098. (doi:10.1103/PhysRevLett.59.2095)
16. Kitaev A, Preskill J. 2006 Topological entanglement entropy. *Phys. Rev. Lett.* **96**, 110404. (doi:10.1103/PhysRevLett.96.110404)
17. Levin M, Wen X-G. 2006 Detecting topological order in a ground state wave function. *Phys. Rev. Lett.* **96**, 110405. (doi:10.1103/PhysRevLett.96.110405)
18. Wildeboer J, Seidel A, Melko RG. 2015 Entanglement entropy and topological order in resonating valence-bond quantum spin liquids. (http://arxiv.org/abs/1510.07682 [cond-mat.str-el])
19. Thouless DJ. 1987 Fluxoid quantization in the resonating-valence-bond model. *Phys. Rev. B* **36**, 7187–7189. (doi:10.1103/PhysRevB.36.7187)
20. Kivelson SA, Rokhsar DS, Sethna JP. 1988 2*e* or not 2*e*: flux quantization in the resonating valence bond state. *Europhys. Lett.* **6**, 353–358. (doi:10.1209/0295-5075/6/4/013)
21. Baskaran G, Anderson PW. 1988 Gauge theory of high-temperature superconductors and strongly correlated Fermi systems. *Phys. Rev. B* **37**, 580–583. (doi:10.1103/PhysRevB.37.580)
22. Fradkin E, Kivelson SA. 1990 Short range resonating valence bond theories and superconductivity. *Mod. Phys. Lett. B* **4**, 225–232. (doi:10.1142/S0217984990000295)
23. Read N, Sachdev S. 1989 Valence-bond and spin-Peierls ground states of low-dimensional quantum antiferromagnets. *Phys. Rev. Lett.* **62**, 1694–1697. (doi:10.1103/PhysRevLett.62.1694)

24. Read N, Sachdev S. 1990 Spin-Peierls, valence-bond solid, and Néel ground states of low-dimensional quantum antiferromagnets. *Phys. Rev. B* **42**, 4568–4589. (doi:10.1103/PhysRevB.42.4568)
25. Senthil T, Vishwanath A, Balents L, Sachdev S, Fisher MPA. 2004 Deconfined quantum critical points. *Science* **303**, 1490–1494. (doi:10.1126/science.1091806)
26. Vishwanath A, Balents L, Senthil T. 2004 Quantum criticality and deconfinement in phase transitions between valence bond solids. *Phys. Rev. B* **69**, 224416. (doi:10.1103/PhysRevB.69.224416)
27. Fradkin E, Huse DA, Moessner R, Oganesyan V, Sondhi SL. 2004 Bipartite Rokhsar Kivelson points and Cantor deconfinement. *Phys. Rev. B* **69**, 224415. (doi:10.1103/PhysRevB.69.224415)
28. Hermele M, Senthil T, Fisher MPA, Lee PA, Nagaosa N, Wen X-G. 2004 Stability of U(1) spin liquids in two dimensions. *Phys. Rev. B* **70**, 214437. (doi:10.1103/PhysRevB.70.214437)
29. Sandvik AW. 2007 Evidence for deconfined quantum criticality in a two-dimensional Heisenberg model with four-spin interactions. *Phys. Rev. Lett.* **98**, 227202. (doi:10.1103/PhysRevLett.98.227202)
30. Read N, Sachdev S. 1991 Large N expansion for frustrated quantum antiferromagnets. *Phys. Rev. Lett.* **66**, 1773–1776. (doi:10.1103/PhysRevLett.66.1773)
31. Jalabert RA, Sachdev S. 1991 Spontaneous alignment of frustrated bonds in an anisotropic, three-dimensional Ising model. *Phys. Rev. B* **44**, 686–690. (doi:10.1103/PhysRevB.44.686.)
32. Wen XG. 1991 Mean-field theory of spin-liquid states with finite energy gap and topological orders. *Phys. Rev. B* **44**, 2664. (doi:10.1103/PhysRevB.44.2664)
33. Sachdev S. 1992 Kagome and triangular-lattice Heisenberg antiferromagnets: ordering from quantum fluctuations and quantum-disordered ground states with unconfined bosonic spinons. *Phys. Rev. B* **45**, 12 377–12 396. (doi:10.1103/PhysRevB.45.12377)
34. Sachdev S, Vojta M. 2000 Translational symmetry breaking in two-dimensional antiferromagnets and superconductors. *J. Phys. Soc. Jpn.* **69**, Suppl. B, 1. (http://arxiv.org/abs/cond-mat/9910231 [cond-mat.str-el])
35. Fradkin E, Shenker SH. 1979 Phase diagrams of lattice gauge theories with Higgs fields. *Phys. Rev. D* **19**, 3682–3697. (doi:10.1103/PhysRevD.19.3682)
36. Alexander Bais F, van Driel P, de Wild Propitius M. 1992 Quantum symmetries in discrete gauge theories. *Phys. Lett. B* **280**, 63–70. (doi:10.1016/0370-2693(92)90773-W)
37. Platé M *et al.* 2005 Fermi surface and quasiparticle excitations of overdoped $Tl_2Ba_2CuO_{6+\delta}$. *Phys. Rev. Lett.* **95**, 077001. (doi:10.1103/PhysRevLett.95.077001)
38. Senthil T, Vojta M, Sachdev S. 2004 Weak magnetism and non-Fermi liquids near heavy-fermion critical points. *Phys. Rev. B* **69**, 035111. (doi:10.1103/PhysRevB.69.035111)
39. Paramekanti A, Vishwanath A. 2004 Extending Luttinger's theorem to $\mathbb{Z}_2$ fractionalized phases of matter. *Phys. Rev. B* **70**, 245118. (doi:10.1103/PhysRevB.70.245118)
40. Yang K-Y, Rice TM, Zhang F-C. 2006 Phenomenological theory of the pseudogap state. *Phys. Rev. B* **73**, 174501. (doi:10.1103/PhysRevB.73.174501)
41. Kivelson SA, Rokhsar DS, Sethna JP. 1987 Topology of the resonating valence-bond state: solitons and high-T_c superconductivity. *Phys. Rev. B* **35**, 8865–8868. (doi:10.1103/PhysRevB.35.8865)
42. Read N, Chakraborty B. 1989 Statistics of the excitations of the resonating-valence-bond state. *Phys. Rev. B* **40**, 7133. (doi:10.1103/PhysRevB.40.7133)
43. Punk M, Allais A, Sachdev S. 2015 A quantum dimer model for the pseudogap metal. *Proc. Natl Acad. Sci. USA* **112**, 9552–9557. (doi:10.1073/pnas.1512206112)
44. Ferrero M, Cornaglia PS, de Leo L, Parcollet O, Kotliar G, Georges A. 2009 Pseudogap opening and formation of Fermi arcs as an orbital-selective Mott transition in momentum space. *Phys. Rev. B* **80**, 064501. (doi:10.1103/PhysRevB.80.064501)
45. Sordi G, Haule K, Tremblay A-MS. 2011 Mott physics and first-order transition between two metals in the normal-state phase diagram of the two-dimensional Hubbard model. *Phys. Rev. B* **84**, 075161. (doi:10.1103/PhysRevB.84.075161)
46. Senthil T, Sachdev S, Vojta M. 2003 Fractionalized Fermi liquids. *Phys. Rev. Lett.* **90**, 216403. (doi:10.1103/PhysRevLett.90.216403)
47. Punk M, Sachdev S. 2012 Fermi surface reconstruction in hole-doped t–J models without long-range antiferromagnetic order. *Phys. Rev. B* **85**, 195123. (doi:10.1103/PhysRevB.85.195123)
48. Chubukov AV, Sachdev S. 1993 Chubukov and Sachdev reply. *Phys. Rev. Lett.* **71**, 3615. (doi:10.1103/PhysRevLett.71.3615)

49. Sachdev S. 1994 Quantum phases of the Shraiman–Siggia model. *Phys. Rev. B* **49**, 6770–6778. (doi:10.1103/PhysRevB.49.6770)
50. Wen X-G, Lee PA. 1996 Theory of underdoped cuprates. *Phys. Rev. Lett.* **76**, 503–506. (doi:10.1103/PhysRevLett.76.503)
51. Ribeiro TC, Wen X-G. 2006 Doped carrier formulation and mean-field theory of the $tt't''J$ model. *Phys. Rev. B* **74**, 155113. (doi:10.1103/PhysRevB.74.155113)
52. Kaul RK, Kolezhuk A, Levin M, Sachdev S, Senthil T. 2007 Hole dynamics in an antiferromagnet across a deconfined quantum critical point. *Phys. Rev. B* **75**, 235122. (doi:10.1103/PhysRevB.75.235122)
53. Kaul RK, Kim YB, Sachdev S, Senthil T. 2008 Algebraic charge liquids. *Nat. Phys.* **4**, 28–31. (doi:10.1038/nphys790)
54. Qi Y, Sachdev S. 2010 Effective theory of Fermi pockets in fluctuating antiferromagnets. *Phys. Rev. B* **81**, 115129. (doi:10.1103/PhysRevB.81.115129)
55. Mei J-W, Kawasaki S, Zheng G-Q, Weng Z-Y, Wen X-G. 2012 Luttinger-volume violating Fermi liquid in the pseudogap phase of the cuprate superconductors. *Phys. Rev. B* **85**, 134519. (doi:10.1103/PhysRevB.85.134519)
56. Ferraz A, Kochetov E. 2013 Gauge invariance and spinon–dopon confinement in the t–J model: implications for Fermi surface reconstruction in the cuprates. *Eur. Phys. J. B* **86**, 512. (doi:10.1140/epjb/e2013-40849-8)
57. Oshikawa M. 2000 Topological approach to Luttinger's theorem and the Fermi surface of a Kondo lattice. *Phys. Rev. Lett.* **84**, 3370–3373. (doi:10.1103/PhysRevLett.84.3370)
58. Shen KM *et al.* 2005 Nodal quasiparticles and antinodal charge ordering in $Ca_{2-x}Na_xCuO_2Cl_2$. *Science* **307**, 901–904. (doi:10.1126/science.1103627)
59. Yang H-B, Rameau JD, Pan Z-H, Gu GD, Johnson PD, Claus H, Hinks DG, Kidd TE. 2011 Reconstructed Fermi surface of underdoped $Bi_2Sr_2CaCu_2O_{8+\delta}$ cuprate superconductors. *Phys. Rev. Lett.* **107**, 047003. (doi:10.1103/PhysRevLett.107.047003)
60. Ando Y, Kurita Y, Komiya S, Ono S, Segawa K. 2004 Evolution of the Hall coefficient and the peculiar electronic structure of the cuprate superconductors. *Phys. Rev. Lett.* **92**, 197001. (doi:10.1103/PhysRevLett.92.197001)
61. Kohsaka Y *et al.* 2007 An intrinsic bond-centered electronic glass with unidirectional domains in underdoped cuprates. *Science* **315**, 1380–1385. (doi:10.1126/science.1138584)
62. Metlitski MA, Sachdev S. 2010 Quantum phase transitions of metals in two spatial dimensions. II. Spin density wave order. *Phys. Rev. B* **82**, 075128. (doi:10.1103/PhysRevB.82.075128)
63. Sachdev S, La Placa R. 2013 Bond order in two-dimensional metals with antiferromagnetic exchange interactions. *Phys. Rev. Lett.* **111**, 027202. (doi:10.1103/PhysRevLett.111.027202)
64. Chowdhury D, Sachdev S. 2014 Density-wave instabilities of fractionalized Fermi liquids. *Phys. Rev. B* **90**, 245136. (doi:10.1103/PhysRevB.90.245136)
65. Chowdhury D, Sachdev S. 2015 Higgs criticality in a two-dimensional metal. *Phys. Rev. B* **91**, 115123. (doi:10.1103/PhysRevB.91.115123)